Acta Acustica united with Acustica
Vol. 99 (2013) 110 – 117
DOI 10.3813/AAA.918594

Recreating the Sound of Stonehenge

Bruno Fazenda, Ian Drumm
Acoustics Research Centre, School of Computing, Science and Engineering, University of Salford, Salford, United Kingdom, M5 4WT. b.m.fazenda@salford.ac.uk

Summary
Stonehenge is the largest and most complex ancient stone circle known to mankind. In its original form, the concentric shape of stone rings would have surrounded an individual, both visually and aurally. It is an outdoor space and most archaeological evidence suggests it did not have a roof. However, its large, semi-enclosed structure, with many reflecting surfaces, would have reflected and diffracted sound within the space creating an unusual acoustic field for the Neolithic Man. The work presented here reports the reconstruction of the acoustic sound field of Stonehenge based on measurements taken at a full size replica in Maryhill, USA. Acoustic measurements were carried out using state-of-the-art techniques and the response collected in both mono and B-Format at various source-receiver positions within the space. A brief overview of Energy Time Curves and Reverberation Time together with a comparison to a recent measurement in the current Stonehenge site is provided. The auralisation process presented uses a hybrid Ambisonic and Wave Field Synthesis (WFS) system. In the electro-acoustic rendering system, sound sources are created as focussed sources using Wave Field Synthesis whilst their reverberant counterpart is rendered using Ambisonic principles. Using this novel approach, a realistic acoustic sound field, as it is believed to have existed in the original Stonehenge monument, can be experienced by listeners. The approach presented, not only provides a valuable insight into the acoustic response of an important archaeological site but also demonstrates the development of a useful tool in the archaeological interpretation of important buildings and heritage sites.

PACS no. 43.55.-n

1. Introduction

The preservation and recreation of the acoustic characteristics of ancient spaces serves various important purposes: It is vital in the reconstruction of theatres [1]; aids in in a more ecologically valid [1] archaeological interpretation of important buildings and heritage sites, some of which may not exist in their original form [2, 3]; and allows experiencing of their soundfields through auralisation which has benefits for public interactive applications. The work presented here reports on the recreation of the acoustic sound field of Stonehenge, a well known pre-historic stone circle situated in Wiltshire, England. Due to its circular shape and the large number of enclosing surfaces, a listener inside the original stone circle would have been presented with an unusual sound field for an outdoor space. However, as it currently stands, the monument is in ruins and only a few of the original stones still remain standing. As such, measuring and experiencing the acoustic sound field within Stonehenge in its final construction phase (ca. 2000 B.C.) has hitherto not been possible.

Figure 1. Photos of sites measured. Left: Stonehenge, right: Maryhill.

A full size identical replica of the Stonehenge monument exists on the banks of the Columbia River in Maryhill, Washington, USA. The stone positions and sizes have been replicated using concrete, the surfaces of which have been shaped in an attempt to simulate stone roughness. The 'stones' in the Maryhill site are, in general, more regular and do not replicate those at Stonehenge in absolute detail (see Figure 1). It may however be argued that some of the more general acoustic effects, such as reflection patterns and reverberation characteristics of Stonehenge, may also be found at Maryhill since the general architectural shape is similar. Significant acoustic differences are most likely to exist at very high frequencies where

Received 4 May 2012,
accepted 17 December 2012.

[1] Ecological validity in this context refers to simulations that emulate the original real life environments in terms of directional and reverberant cues.

the wavelength becomes comparable to the differences in stone profile found at each site ($\approx$ 30 cm; $f \approx 11$ kHz; $c = 340$ m/s). At this range of frequencies, particular diffusion and diffraction effects are not replicated at Maryhill. A series of acoustic measurements based on B-Format impulse responses has been carried out at the Maryhill site in order to obtain data for auralisation of the space using a hybrid approach that combines Wave Field Synthesis (WFS) and Ambisonic reproduction.

This paper describes the measurement and auralisation process and is organised as follows: Section 2 gives a brief overview of Stonehenge including brief results of acoustic measurements taken at the site; section 3 discusses measurement and results for the acoustic response of the Maryhill site; section 4 discusses the rendering method and its validation; section 5 describes the production of a soundscape that has been used in public presentations of the system; a summary of this work is finally presented in section 6.

2. Stonehenge

The Stonehenge monument is characterised by concentric stone rings of various sizes. The outer circle is composed of 30 upright sarsen stones, 17 of which are still standing (shaded in Figure 2). The tops of the upright sarsen stones were originally linked by a horizontal lintel ring. Inside the sarsen ring there was a 2^{nd} circle of smaller blue stones. The 5 large trilithons, arranged in a horseshoe shape of blue stones and another series of head-height bluestones arranged in an oval shape, form the 3^{rd} inner semi-enclosure. More detailed information about the site and its archaeological study can be found in [4]. Acoustic measurements have been carried out inside the Stonehenge monument using the balloon burst method [5] since no mains energy or other impulse generating methods were allowed on site. Envelope-Time Curves (ETC) have been determined from measured impulse responses (IR) as follows. Given a time domain impulse response $h(t)$, the linear scale envelope time curve can be obtained from

$$e(t) = \left| h(t) + \mathrm{j}\hat{h}(t) \right|, \tag{1}$$

where $\hat{h}(t)$ is the Hilbert transform of the signal $h(t)$ given by

$$\hat{h}(t) = \frac{1}{\pi} \int_{-\infty}^{\infty} \frac{h(\tau)}{t - \tau} \,\mathrm{d}\tau. \tag{2}$$

Assuming $h(t)$ denotes acoustic pressure, the Heyser energy time curve in decibel scale normalised to the direct source, can be obtained from

$$ETC(t) = 20 \log \left(\frac{h(t)}{h_{direct}} \right). \tag{3}$$

The ETC obtained for source and receiver in the centre of Stonehenge (indicated respectively as M1 and 1 in Figure 2) is shown in Figure 3.

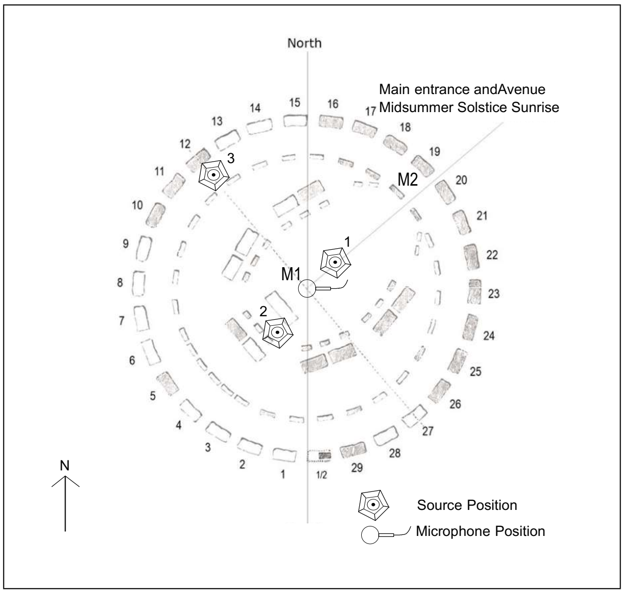

Figure 2. Diagram of Stonehenge circle. Receiver position is marked as M1 in the centre. Source positions used for the acoustic measurements are indicated as 1, 2 and 3.

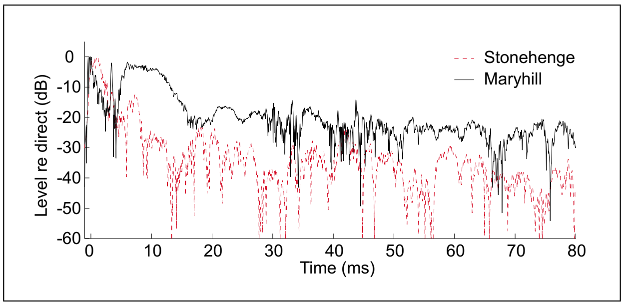

Figure 3. ETCs derived from single channel impulse responses. The response shown corresponds to source at position 1 in Figure 2 and the receiver at the centre. Stonehenge (dashed) and Maryhill (solid) results are provided.

The ETC response measured at the centre of the Stonehenge monument shows a few specular reflections although, depending on which subjective data is used [6, 7], they barely rise above the reflection detection threshold. Anecdotal evidence from the measurement visit whilst standing inside the stone circle revealed a faint slap-back type echo arising mainly from the intact portion of the outer sarsen ring, where the longer time of arrival (>40 ms) allows the perception of a faint reflection.

The reverberation times for measurements on site have been determined according to ISO3382. Various source and receiver positions were used. Because the balloon burst method is associated with a very low signal to noise ratio, the portion of decay curve used to extrapolate RT from the Stonehenge data has been truncated between −5 dB and −15 dB for frequencies below 200 Hz and between −5 dB and −25 dB for frequencies above. T30 data has been used for the Maryhill measurements. Results are shown in Figure 4. As expected from an outdoor site, the RT values for Stonehenge are quite low, averaging 0.4 sec-

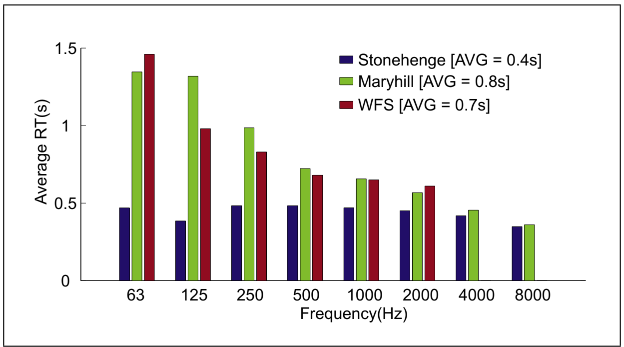

Figure 4. Reverberation Times for acoustic measurements at Stonehenge and Maryhill sites (left and centre bars); and for the Wave Field Synthesis/Ambisonic hybrid system used to recreating its acoustic response (right bars). RT figures for each octave band in the measured data were obtained from the arithmetic average of various source and receiver positions. RT for each octave band in the rendering system has been obtained from a single FDTD simulation. RT values indicated in the legend correspond to wideband averages.

onds for the 500 Hz and 1 kHz octave bands (0.4 s in the 63 Hz to 8 kHz range).

These results confirm the expected notion that Stonehenge, in its current form, has few noteworthy acoustic features. Notwithstanding, in its final stage of construction, circa 2000 B.C., it is likely that the sound field within Stonehenge would have revealed a different character. Indeed, one could argue that the large number of enclosing stones, of different sizes and shapes and at different distances, would have created significant levels of diffusion. Specular reflections, such as those measured in the current Stonehenge, would have been replaced by multiple reflection paths arriving in succession at a listener position. It is also likely that, enclosed by many reflective surfaces, the space would have sustained a significant level of reverberation that might have been unusual for people visiting the site.

3. Maryhill

Given the Stonehenge site is in ruins, a faithful model of its acoustic response is required to obtain reliable acoustic measurements that may provide an indication of the acoustic characteristics of such a building. It is granted that a number of modelling techniques are available to predict the acoustic behaviour of spaces, for example [8, 9, 10]. Although such digital techniques are extremely powerful at generating predictions of the acoustic sound field, they are also dependent on the accuracy of the CAD model used and are not totally free of issues and imprecisions [11, 12]. A more traditional method, based on the use of physical models, has long been a robust and accepted practice in acoustic design and research, only recently getting replaced by digital models [13, 14]. It is thus justifiable that the use of a physical model is an acceptable method to study the acoustic response of a space and consequently to create an auralisation of the sound-field within it.

An identical replica of the Stonehenge monument, as it is believed to have existed at around 2000 B.C., exists in Maryhill, Washington state, USA. The Maryhill Stonehenge is a full size, physical model of Stonehenge, built in 1929 as a memorial to the soldiers of the First World War. This physical model provides the closest physical representation of the acoustic sound field present during the last phase of the construction of Stonehenge (see [4] for an archaeological and historical recount of the construction phases at Stonehenge). This has thus been exploited to obtain acoustic measurements for analysis of the acoustic response and to recreate an auralisation of its sound field.

Techniques for measuring the acoustic characteristics of performance spaces have been widely reported [15, 16]. ISO3382 sets the standard for such measurements although it does not acknowledge or utilize the advantages brought about by the use of pressure-particle velocity probes such as the Soundfield microphone (www.soundfield.com). The use of Soundfield microphones for capturing spatial sound properties of a space and the resulting B-Format output for rendering through varied electroacoustic formats (binaural, stereo, 5.1 and ambisonic) are now becoming ubiquitous in measurement-to-auralisation work such as the one presented here (see for example [2, 17, 18]).

The measurement method used here follows standard procedures established in the work referenced above. In particular, a dodecahedron source was paired with a subwoofer to adequately cover the audio frequency range between 40 Hz and 10 kHz with an omnidirectional polar response. The excitation signal used was a 10 second log-sweep. The acoustic response of the space was captured using both an omnidirectional reference microphone (to obtain conventional impulse response and derive standard acoustic measures as prescribed in ISO3382) and a Soundfield ST250 microphone to capture the B-Format impulse responses. A first order B-Format signal consists of 4 spatially coincident signals corresponding to one omnidirectional pressure signal, W, and 3 orthogonal figure-of-eight pressure gradient signals, X,Y and Z, directed as front-back, left-right and up-down respectively (more details on B-Format technology can be found at www.soundfield.com). The B-Format impulse responses provide a means of extracting monaural acoustic parameters of the space from the W signal and spatial information about the time and level of arrival of reflected energy from the X,Y,Z pressure gradient signals.

The subwoofer was placed on the floor and the dodecahedron was placed directly above it at a height of approximately 1.6 m. Microphones were positioned at an average standing head height of 1.6 m. All measurements presented for the Maryhill site were obtained using WinMLS software, a modern personal computer and a Focusrite Saffire Pro 10 soundcard set to sample at 48 kHz with 16 bit. As measurements were taken outdoors, power was provided via a combustion generator where due care was taken to minimise noise contamination onto the measured responses. Similarly, and due to proximity of roads, environmental conditions and public access to the site, every measurement was checked for adequate signal to noise ratio to ensure validity of data.

Maryhill measurements show an average RT of 0.7 seconds in the 500 Hz to 1 kHz frequency range (0.8 seconds in the 63 Hz to 8 kHz range). The ETC for a source placed in the centre of the space and obtained with a single channel reference measurement also in the centre is shown in Figure 3 (solid line). In comparison to the measurement taken at Stonehenge in identical source-receiver relationship (Figure 3-dashed line), it is clear that the Maryhill monument exhibits significant reflected energy. Interestingly, there are no defined specular reflections suggesting the space might support an acoustic sound field more similar to diffuse conditions. Reverberation times for the Maryhill site are indicated in Figure 4. As expected, the values for RT are significantly higher than those measured at Stonehenge since, at least in the horizontal axis, the larger number of surrounding stone surfaces offers a more enclosed environment. This effect is clearly perceived as one walks into the space and this is portrayed quite clearly in the auralisation work reported here.

The auralisation of the space, described in detail in section 4, was performed using measurements taken at a single receiver position, at the centre of the stone circle as indicated in Figure 2. Three source positions were used to independently excite the space at various points. These are also indicated in Figure 2. Using the Soundfield microphone, B-Format impulse responses were acquired for each of the source positions. Each of these measurements provides 4 channels of data where the acoustic response of the environment at the measurement position is acquired. An example of an orthogonal impulse response measured in the centre of the Maryhill monument is shown in Figure 5. The W signal corresponds to the pressure component (omnidirectional). The X and Y signals contain the front/back and left/right orthogonal components respectively. The Z component, corresponding to height information, is not displayed. This latter component is not used in the rendering system since the acoustic sound field in this dimension is mainly absorbent – the space has no roof; floor reflections appear in X and Y channels as weaker, horizontal, reflection energy. Furthermore, the wave field synthesis system developed does not reproduce height information and could not therefore reproduce this dimension.

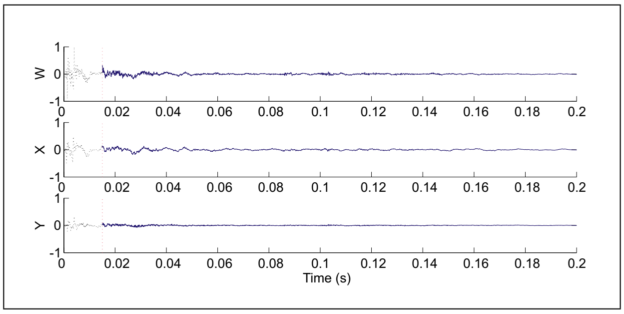

Figure 5. Orthogonal Impulse Responses measured in Maryhill (a full size identical replica of Stonehenge). Only W,X and Y signals are represented. Direct and reflected sound regions are plotted in different line styles.

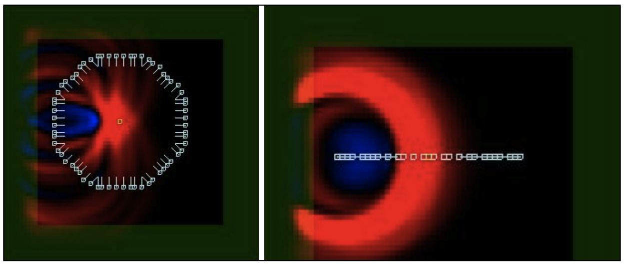

Figure 6. Focussed source using the Wave Field Synthesis reproduction system. An FDTD model has been used to recreate the electro-acoustic system for illustrative purposes. Left: Top view, right: Side view.

4. Electro-acoustic rendering system

The rendering system developed emphasises two important aspects of aural perception: the correct localisation of a physical sound source and its embedding in an ecologically valid acoustic environment. It is thus expected that the rendering system is able to reproduce both the correct directional cues for the rendered sources as well as their interaction with the acoustic characteristics of the space they inhabit. In doing so, an immersive and realistic auralisation of the space is obtained. In the case presented here, the aim of the electro-acoustic system is to render sound sources and their reflected counterparts (early reflections and reverberation) as would be experienced within the original Stonehenge. The method developed is novel yet based on a simple principle:

- Dry sound sources are rendered as focussed sources using wave field synthesis (WFS) principles. Focussed sources are explained in more detail in section 4.1. The system allows real time movement of these sources.
- The acoustic response of the space is obtained through convolution of the dry source signals and the orthogonal impulse responses obtained within it. The resulting IRs have been manipulated to remove the direct sound information since this has already been rendered into the auralisation space in the form of a focussed source.

A listener within the electro-acoustic rendering system is thus subjected to the correct directional cues generated from the reconstructed wavefronts for the focused sources and the ecologically valid environmental reflections of the space. The rendering system used here has been fully developed within the Acoustics Research Centre at the University of Salford and is based on commercially available hardware comprised of 64 audio channels that drive an octagon shaped array of 64 loudspeakers (see Figure 6). The WFS, ambisonic and control algorithms are based on our own developed C++/C# /WASAPI software application.

4.1. Reproducing focussed sources in WFS

The theoretical basis for wave field synthesis was developed in the frequency domain [19, 20] to demonstrate how a soundfield within a volume can be constructed from arrays of monopole or dipole sources on enclosing 2D surfaces. WFS employs the Huygens principle which essentially states that wavefronts can be created by the cumulative effect of secondary sources just behind them. Given a plane of monopole sources the pressure at the receiver point in the volume can be predicted by adding secondary source contributions using a half space simplification of the Kirchhoff-Helmholtz integral. Therefore, in theory, desired wavefields within a volume can be constructed from a set of enclosing surfaces of secondary sources. Considering a virtual source located in space such that its position vector is r_s, the pressure at r_v as a function of frequency ω can be considered as a sum of contributions of a driving function at secondary source (i.e. loudspeaker) positions r_l such that

$$p_r(\omega) \propto \int_S D \frac{\mathrm{e}^{-\mathrm{j}k|r_v - r_l|}}{|r_v - r_l|} \, \mathrm{d}S. \tag{4}$$

Typically the driving function includes a window a to ensure only forward propagating waves reach the listener and a stationary phase approximation to represent vertical contributions at a given loudspeaker since linear arrays (not planes) are used [21, 22]. Driving functions for wavefields in arbitrary shaped arrays can be specified for plane wave and spherical wave sources [23]. Equation (5) is the driving function for a spherical wave. The S term represents the sound signal to be rendered, n is the direction vector of the loudspeaker and $s = \mathrm{j}\omega$.

$$D = -2a\sqrt{2\pi \left| r_l - r_{ref} \right|} \frac{(r_l - r_s)^T n}{(r_v - r_l)} \frac{1}{\sqrt{c}} \cdot \left(s + \frac{c}{|r_l - r_s|} \right) \frac{1}{s} \mathrm{e}^{-\mathrm{j}k|r_l - r_s|} S(\omega). \tag{5}$$

In practice, virtual sources (herewith named *focussed sources*) are positioned within the world space coordinate system and their contributions to the respective driving functions are evaluated in the time domain, hence rendered by setting amplitudes, delays and coefficients of an FIR (or IIR) filter (which is used to account for the source spectra being a function of r_s). The WFS part of the system is thus able to recreate the wavefronts of multiple arbitrarily positioned virtual sources both outside and within the confines of the speaker array thus emulating the distribution of sound waves in a volume as would be experienced by a user at any given position within that volume. As such, WFS does not require users to remain at a designated sweet spot and movements of both source and listener are allowed whilst maintaining the correct directional cues.

4.2. 'Reverberant Tails' in Ambisonic Reproduction

In order to place the dry focussed sources within the rendering of Stonehenge , they have to be convolved with the measured orthogonal IRs thus providing a spherical harmonic decomposition of these sources in the reverberant sound field. However, correct integration with the rendered focussed sources provided by the WFS system requires that only the early reflections and reverberation of the space, herewith named reverberation tails, are reproduced by the ambisonic system. It follows that the direct sound and first reflection must be identified in the impulse responses.

The identification of the onset on the impulse responses was performed using a technique based on measuring the variation of temporal energy contained in the impulse response and finding where the energy ratio of consecutive analysis windows is maximum [24]. The impulse response is then trimmed to the index corresponding to its onset. The reflection onset times (ROT) are then obtained through a running kurtosis analysis as established in [25]. This analysis is carried out on the W signal since this channel, corresponding to the omnidirectional response, contains all reflections at their maximum amplitudes. ROT_1 is then used to determine the point before which each of the W,X and Y impulse responses must be padded with zeros to remove the direct sound. Zero padding ensures that the correct propagation time between source and receiver are maintained in the data series. The resultant impulse response waveforms can be seen in Figure 5. The initial portion, plotted in a dashed black line, corresponds to the direct sound. The remaining data points, plotted in a solid blue line, are the reverberant tails containing early reflections and reverberation. Note that the propagation time from the direct sound to ROT_1 is also included in the data vectors for subsequent convolution with the desired source signal.

The reverberant tails are rendered simultaneously through the same system but decoded as Ambisonic sources by applying Gerzon's equations [26] across all loudspeakers. For each loudspeaker, the relative contributions of X and Y are set as functions of the angle between r_l-r_s and n. Due to the underlying ambisonic theory and its first order limitation in this case, the ambisonic cues are only rendered correctly to a centrally placed listener. Thus, for a centrally placed listener heading in any direction, the rendered source cues (time, direction and amplitude) are correct for sources placed at the same positions as those used to measure the IRs in the physical space (source positions 1,2 and 3 in Figure 2). If real time movement of the focused sources is required or the listener moves within the rendering environment, the early reflection cues will no longer maintain their corrected cues unless their corresponding orthogonal IRs are rotated and the amplitude of individual reflections manipulated accordingly. Reverberant cues, per definition, will not make a significant contribution to subjective source localisation. It is reasonable to argue that, if the focussed source cues are correctly maintained, they will dominate over the early reflection and reverberation cues and thus maintain accurate source localisation and realism. Indeed this was the case at a few event demonstrations of the system.

To deal with the case of moving listener or sources, an interpolation between a comprehensive grid of source-receiver IRs would be required to maintain a physically accurate representation of the reflection profile of the space for each desired position. To obtain this grid, extensive acoustic measurement in physical models or comprehensive model prediction of the acoustic sound-field would be require. Whether a large number of acoustic measurements or state-of-the-art acoustic digital models are prescribed to deal with this problem, these would invariably lead to considerable costs in operational efficiency of the rendering system and was thus not attempted in this work.

4.3. Validation of the rendering system

To validate the method described in this paper and to provide illustrative results of the system performance, a Finite Difference Time Domain (FDTD) emulation of the WFS/Ambisonic electro-acoustic system has been developed. The FDTD model avoids issues which ensue from measurements of the physical reproduction system directly. The FDTD model allows a validation of the integration of the focussed sources reproduced using WFS with the reverberant tails reproduced through ambisonic decoding.

Though originally developed for computational electrodynamics [27], FDTD is useful for modelling broadband sound propagation phenomena [10] and can be adapted to model sound within complex environments that include arbitrarily shaped frequency dependent boundaries [28]. The acoustic implementation of FDTD considers sound propagation as coupled equations (6) and (7):

$$\frac{1}{K}\frac{\partial p}{\partial t} = -\nabla w, \tag{6}$$

$$\rho\frac{\partial w}{\partial t} = -\nabla p, \tag{7}$$

where p is pressure, w is particle velocity, ρ is the density of medium and K its bulk modulus. Writing equations (6) and (7) in discrete centre-difference forms yields equations (8), (9), (10) and (11) where i, j and k represent grid locations and n represents time steps.

$$w_x^{n+1}\left(i+\frac{1}{2}, j, k\right) = w_x^{n}\left(i+\frac{1}{2}, j, k\right) - \frac{\delta t}{\rho\delta x}\left\{p^{n+\frac{1}{2}}(i+1, j, k) - p^{n+\frac{1}{2}}(i, j, k)\right\}, \tag{8}$$

$$w_y^{n+1}\left(i+\frac{1}{2}, j, k\right) = w_y^{n}\left(i+\frac{1}{2}, j, k\right) - \frac{\delta t}{\rho\delta y}\left\{p^{n+\frac{1}{2}}(i+1, j, k) - p^{n+\frac{1}{2}}(i, j, k)\right\}, \tag{9}$$

$$w_z^{n+1}\left(i+\frac{1}{2}, j, k\right) = w_z^{n}\left(i+\frac{1}{2}, j, k\right) - \frac{\delta t}{\rho\delta z}\left\{p^{n+\frac{1}{2}}(i+1, j, k) - p^{n+\frac{1}{2}}(i, j, k)\right\}, \tag{10}$$

$$p^{n+\frac{1}{2}}(i, j, k) = p^{n-\frac{1}{2}}(i, j, k) - K\delta t\left\{\begin{array}{l}\frac{w_x^n\left(i+\frac{1}{2},j,k\right)-w_x^n\left(i-\frac{1}{2},j,k\right)}{\delta x}+\ldots\\ \frac{w_y^n\left(i+\frac{1}{2},j,k\right)-w_y^n\left(i-\frac{1}{2},j,k\right)}{\delta y}+\ldots\\ \frac{w_z^n\left(i+\frac{1}{2},j,k\right)-w_z^n\left(i-\frac{1}{2},j,k\right)}{\delta z}.\end{array}\right. \tag{11}$$

Hence, sound propagation in the medium can be represented as interleaved 3D grids of pressure and velocities respectively, with neighbouring pressure and velocity nodes separated by a half step in time and space. To avoid reflections at grid terminations, perfectly matched layers (PMLs) [29] are implemented to introduce gradual absorption whilst keeping the impedance constant. By adding or setting pressures within specified grid positions various source types can be emulated.

The method was adapted for emulating the hybridised WFS/Ambisonic rendering of Stonehenge by placing 64 hard sources within the pressure grid at positions corresponding to loudspeaker positions and hence setting summed pressures as functions of time accordingly. Figure 6 shows the source layout. Detectors can be added at the desired listener positions to record pressure and particle velocity responses. The technique can be extended to model the sound system's mediating environment and listener's head and body shape [30].

4.3.1. 'Dry' focussed sources

One often overlooked but very important aspect of a convincing auralisation is the correct representation of source wavefronts. The advantages of reproducing the dry focussed sources using WFS is that the correct wavefront is generated for listeners positioned anywhere within the rendering space (except between the rendered source and the main loudspeakers responsible for generating it due to preecho effects). The rendering of a focused source within the electro-acoustic system is demonstrated in Figure 6, which displays a time frame when the focussed source just to the left of the listener position (centre of the array) reaches the listener. The compression and rarefaction zones of the wavefront can clearly be seen as they progress from left to right across the listening area. If only this focussed source is considered, a listener can freely move in an area around it whilst still localising the source at the defined position. This perceptual effect is crucial in conveying a realistic aural representation of the sound source [31]. In the system presented, focussed sources can be generated at various positions within the space and moved in real time. Listeners may also move relative to the source position whilst the source position directional cues are maintained.

4.3.2. Reverberant cues

For a listener positioned at the centre of the electro-acoustic system the correct reverberant cues may be created using ambisonic technology as described in 4.2. The FDTD modelled output from the system is shown in Figure 7. The detector position is defined at the centre of the loudspeaker array where directional cues decoded from the B-Format measurements system will be correct if the

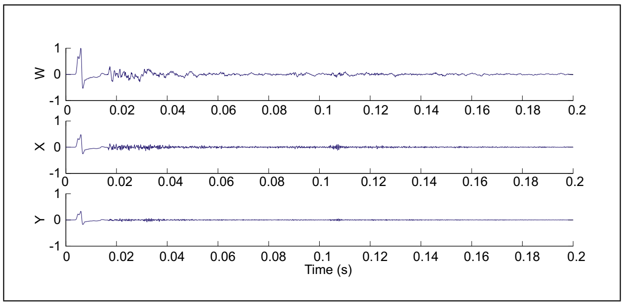

Figure 7. Orthogonal impulse responses for a centrally placed receiver in the hybrid WFS/Ambisonic rendering system. Responses contain both direct and reflected sound. Source and receiver relationship is identical to measurement in Figure 5.

source position matches those used for measuring the B-Format responses in the physical space. For validation purposes, the same source/receiver relationship as shown in Figure 5 has been used. The FDTD grid has been excited using a point source. The orthogonal responses shown in Figure 7 contain both the direct sound, which is rendered as a focussed source as described in 4.3.1, and the reverberant tail, which is rendered using correct decoding equations for each of the 64 loudspeakers in the system. The RT presented by the rendering system when configured to reproduce one of the sources within Stonehenge has been determined from the W (omnidirectional) signal and is shown in Figure 4. The obtained values for RT are comparable to what was measured on site. Some differences are observed which can be explained by the fact that a single source/receiver position for the modelled response is being used rather than an average of various measurements as is the case in the physical measurement data. The results demonstrate that a listener within the rendering system is presented with a soundfield similar to that existing in the real space.

5. Creating the soundscape within Stonhenge

For public presentation, a folk ensemble comprised of two singers, one percussion instrument and a choir was rendered in the system. Source positions marked 2 and 3 in Figure 2 were selected for the two singers since the orthogonal IRs obtained at these positions contain the physically correct spatial cues. Given the limited number of measured source positions, two extra source positions were generated by inverting the pressure gradient sensitive channels of the corresponding IRs prior to convolution. I.e. two further source positions, diametrically opposite positions 2 and 3, were generated by inverting the respective Y and X signals of the corresponding original B-Format IRs. The authors are aware that this latter technique will not represent the acoustic environment accurately but rather flip it in terms of side to side or front to back. It is nevertheless a complementary tool that may be used to obtain more source positions when only a few measurements are available, without introducing gross inaccuracies. Furthermore, editing the temporal and amplitude response of reflections in the obtained IRs would allow further manipulation of the resulting directional cues and reverberation characteristics. Such techniques, as are already available in convolution reverb applications [32], will not be entirely accurate as they distort the physical characteristics of the space but are available to add flexibility to the method. The perceptual benefits of such techniques when compared to the more costly option of comprehensive B-Format IR measurement grids and associated interpolations is an issue for further investigation.

6. Summary

The work presented here describes a set of acoustic measurements and the development of an electro-acoustic rendering system to recreate an auralisation of the Pre-Historic monument Stonehenge as it is believed to have existed around 4000 years ago.

A brief overview of acoustic measurements taken at Stonehenge and at a full size identical and complete replica of it at Maryhill, USA, has been reported. It has been shown that the acoustic sound field currently present at the Stonehenge monument reveals a few weak specular reflections and weak acoustic reverberation. This is naturally associated with the fewer stones still standing at the site and a section providing a clear propagation path between the centre and the outer sarsen circle. At Maryhill, echo and focusing effects that could have been expected from the circular shape of the structure, are actually very weak and present no such acoustical problems. This is due to the peculiar shape of the site with various concentric circles of stones and the stone-gap-stone arrangement, providing a high degree of sound scattering and creating conditions where the arrival of reflected energy is evenly spread out in time rather than at the defined intervals typical of specular reflections. The larger number of stones arranged in concentric circles helps to retain reverberant energy within the space even without the presence of a roof. The site's response is thus characterised by a short but noticeable reverberation with no evidence of echoes.

The rendering system presented is a novel concept that brings together wave field synthesis and ambisonic reproduction techniques. Numerical validation of the method has been presented using a Finite Difference Time Domain model of the rendering system. The correct generation of focussed sources within the rendering space has been demonstrated. The acoustic response obtained when modelling a source in Stonehenge through the rendering system is similar to the conditions found in the measured physical model at Maryhill.

The approach presented not only provides a valuable insight into the acoustic response of an important archaeological site but also demonstrates the development of a useful tool in the archaeological interpretation of important buildings and heritage sites, some of which may not exist in their original form.

The rendering system has been setup at public events and may be experienced at the Acoustics Research Centre at the University of Salford. Auralisations using a similar binaural/ambisonic hybrid technique and FDTD animations of the rendering principles are available at www.acoustics.salford.ac.uk/res/fazenda/acoustics-of-stonehenge/.

Acknowledgement

We thank the Schools of Computing and Engineering and Music, Humanities and Media at the University of Huddersfield for supporting the measurement trips; the Maryhill Museum of Art for access to the Maryhill site; and English Heritage for providing access to the Stonehenge site. Thanks also to Dr Rupert Till who has been involved in the measurements and discussions about the acoustic response of both sites.

References

[1] A. Farina, L. Tronchin: Advanced techniques for measuring and reproducing spatial sound properties of auditoria. International Symposium on Room Acoustics: Design and Science (2004).

[2] D. Murphy: Archaeological acoustic space measurement for convolution re-verberation and auralization applications. Conference on Digital Audio Effects (DAFXÕ06), 2006.

[3] D. Lubman: Acoustical solutions to archaeological mysteries at chichen itza's temple of kukulkan. The Journal of the Acoustical Society of America **128** (2010) 2329.

[4] M. PEARSON: Stonehenge: Exploring the greatest stone age mystery. Simon & Schuster (2011).

[5] J. Patynen, B. Katz, T. Lokki: Investigations on the balloon as an impulse source. The Journal of the Acoustical Society of America **EL129** (2011).

[6] R. Litovsky, H. Colburn, W. Yost, S. Guzman: The precedence effect. The Journal of the Acoustical Society of America **106** (1999) 1633–1654.

[7] S. E. Olive, F. E. Toole: The detection of reflections in typical rooms. J. Audio Eng. Soc **37** (1989) 539–553.

[8] M. Vorlander: Simulation of the transient and steady-state sound propagation in rooms using a new combined ray-tracing/image-source algorithm. The Journal of the Acoustical Society of America **86** (1989) 172–178.

[9] D. Botteldooren: Finite-difference time-domain simulation of low-frequency room acoustic problems. The Journal of the Acoustical Society of America **98** (1995) 3302.

[10] J. Maloney, K. Cummings: Adaptation of fdtd techniques to acoustic modeling. 11th Annual Review of Progress in Applied Computational Electromagnetics, 1995, 724–731.

[11] K. Kowalczyk, M. van Walstijn: Formulation of locally reacting surfaces in fdtd/k-dwm modelling of acoustic spaces. Acta Acustica united with Acustica **94** (2008) 891–906.

[12] H. Jeong, Y. Lam: Source implementation to eliminate low-frequency artifacts in finite difference time domain room acoustic simulation. The Journal of the Acoustical Society of America **131** (2012) 258.

[13] J. Picaut, L. Simon: A scale model experiment for the study of sound propagation in urban areas. Applied Acoustics **62** (2001) 327–340.

[14] M. Kleiner, B.-I. DalenbŁck, P. Svensson: Auralization-an overview. J. Audio Eng. Soc **41** (1993) 861–875.

[15] R. Pompoli, N. Prodi: Guidelines for acoustical measurements inside historical opera houses: procedures and validation. Journal of sound and vibration **232** (2000) 281–301.

[16] A. Farina, R. Ayalon: Recording concert hall acoustics for posterity. 24th AES Conference on Surround Sound, Techniques, Technology and Perception, 2003.

[17] D. Murphy: Multi-channel impulse response measurement, analysis and rendering in archaeological acoustics. 119th Audio Engineering Society Convention, 2012.

[18] V. Merimaa, Juha; Pulkki: Spatial impulse response rendering i: Analysis and synthesis. J. Audio Eng. Soc **53** (2005) 1115–1127.

[19] A. Berkhout, D. de Vries, P. Vogel: Acoustic control by wave field synthesis. The Journal of the Acoustical Society of America **93** (1993) 2764.

[20] A. J. Berkhout: A holographic approach to acoustic control. J. Audio Eng. Soc **36** (1988) 977–995.

[21] P. Vogel: Application of wave field synthesis in room acoustics. Thesis **Delft University of Technology** (1993).

[22] E. W. Stuart: Application of curved arrays in wave field synthesis. Audio Engineering Society Convention 100, 5 1996.

[23] S. Spors, A. Kuntz, R. Rabenstein: An approach to listening room compensation with wave field synthesis. Audio Engineering Society Conference: 24th International Conference: Multichannel Audio, The New Reality, 6 2003.

[24] G. Defrance, L. Daudet, J. Polack: Finding the onset of a room impulse response: Straightforward? The Journal of the Acoustical Society of America **124** (2008) EL248–EL254.

[25] J. Usher: An improved method to determine the onset timings of reflections in an acoustic impulse response. The Journal of the Acoustical Society of America **127** (2010) EL172–EL177.

[26] M. A. Gerzon: Periphony: With-height sound reproduction. J. Audio Eng. Soc **21** (1973) 2–10.

[27] K. Yee: Numerical solution of initial boundary value problems involving maxwell's equations in isotropic media. Antennas and Propagation, IEEE Transactions on **14** (1966) 302–307.

[28] I. Drumm: Importing arbitrary complex objects with a fdtd based prediction application. Institute of Acoustics Spring Conference, 2008.

[29] J. Berenger: A perfectly matched layer for the absorption of electromagnetic waves. Journal of computational physics **114** (1994) 185–200.

[30] I. Drumm, R. Oldfield: The prediction of synthesised wavefields within realistic room acoustics scenarios. Proceedings of 20th International Congress on Acoustics (2010).

[31] J. Blauert: Spatial hearing-revised edition: The psychophysics of human sound localization. MIT press, 1996.

[32] R. Ben-Hador, I. Neoran: Capturing manipulation and reproduction of sampled acoustic impulse responses. Proc. Audio Eng. Soc. 117th Conv., paper (2012).